UNIVERSITY AT STONY BROOK

CEAS Technical Report 730

RESISTIVE GRIDS IN EARLY-VISION CHIPS: n-DIMENSIONAL NONLINEAR NONUNIFORM GROUNDED GRIDS

Victor A. Chang and Armen H. Zemanian

This work was supported by the National Science Foundation under Grant MIP-9423732.

September 5, 1996

Resistive Grids in Early-Vision Chips: n-Dimensional Nonlinear Nonuniform Grounded Grids *

Victor A. Chang and Armen H. Zemanian

Department of Electrical Engineering
University at Stony Brook
Stony Brook, N.Y 11794-2350, U.S.A
e-mail: vchang@sbee.sunysb.edu , zeman@sbee.sunysb.edu
FAX: (516) 632-8494

Abstract

An iterative method is devised for determining the DC behavior of the resistive grids commonly found in vision chips and more generally the voltage-current regime of an n-dimensional nonlinear nonuniform grounded grid, which may be either finite or infinite. The grid may be triangular (also called hexagonal), rectangular, or more generally automorphic under every shift mapping of the nodes, but it is locally finite. The analysis is accomplished under conditions restricting the nonlinearity and nonuniformity sufficiently to allow the operator arising from a nodal analysis to be decomposed into the sum of a Laurent operator and a nonlinear operator, which in turn can be rearranged into a contraction mapping. A similar analysis, wherein the Laurent operator is replaced by a circulant matrix, works for a finite grid.

1 Introduction

A structure appearing in early vision chips is a triangular (also called hexagonal) grid of resistors whose nodes are excited by current sources due to an image falling upon an

*This work was supported by the National Science Foundation under Grant MIP-9423732.

array of photosensitive devices (see [2] and the references therein). The grid is perforce finite, and the resistors are in general nonlinear and nonidentical, that is, the grid's graph is uniform (i.e., automorphic under all shift mappings of the nodes); but its electrical elements have nonlinear characteristics which vary in general from place to place. An outstanding problem is the determination of the voltage-current regime for a given set of excitations. Since early-vision grids are large, standard nonlinear solution techniques are onerous and time-consuming for this purpose. Another approach is to replace the grid by an infinite linear uniform one, in which case the solution is easily obtained by using Laurent operators [6, Sections 7.1 to 7.3] or alternatively the z-transform. The use of an infinite grid is usually acceptable if the behavior at more central points of the grid is of primary interest. The assumptions of linear and uniform element characteristics are less acceptable.

In this paper we present a new iterative method for solving an infinite grid whose nonlinearities and nonuniformities are not overly severe. This allows a nodal analysis to be solved by means of a Laurent operator and a contraction mapping by first approximating the structure by a linear uniform grid and then taking the nonlinear and nonuniform deviations from the appproximation into account through the contractive mapping. The result will be a method of solution that is much more efficient than would be a standard technique for solving a large nonlinear network. Moreover, the technique can be modified to make it suitable for a nonlinear nonuniform finite grid, where now the Laurent operator is replaced by a finite matrix and the nonlinearities and nonuniformities are again encompassed within a contraction mapping. Another result of this work is that we establish herein a class of networks with possibly nonmonotone characteristics having unique operating points.

In the following, $\mathbf{Z}^n$ denotes the set of n-dimensional vectors whose entries are integers; thus, $j \in \mathbf{Z}^n$ if and only if $j = (j_1, \ldots, j_n)$ where each j_k is an integer. Also $\mathbf{0}$ will denote the origin $(0, \ldots, 0)$ of $\mathbf{Z}^n$ whatever the choice of n may be.

2 The General n-dimensional Grid

We will use an indexing system that works for both finite and infinite grids. Consider a grid of n dimensions containing nodes that are indexed by $j = (j_1, j_2, \ldots, j_n) \in \mathbf{B} \subseteq \mathbf{Z}^n$ plus an

additional ground node. For simplicity, we will assume that the k-th dimension of $\mathbf{B}$ is a sequence of M_k consecutive integers. Let $\mathbf{P}$ be a finite subset of $\mathbf{Z}^n$ that satisfies the following three conditions:

a. $\mathbf{0} \notin \mathbf{P}$.

b. If $p = (p_1, p_2, \ldots, p_n) \in \mathbf{P}$, then $-p = (-p_1, -p_2, \ldots, -p_n) \in \mathbf{P}$.

c. $|p_k| < M_k$, where p_k is the k-th component of an element of $\mathbf{P}$.

Also, let $\oplus$ be a binary operator. The algebraic structure $(\mathbf{B}, \mathbf{P}, \oplus)$ satisfies the following condition:

$$b \oplus p = p \oplus b \in \mathbf{B} \tag{1}$$

for all $b \in \mathbf{B}$ and $p \in \mathbf{P}$, where $\oplus$ denotes componentwise addition that is either conventional addition or modulus-M_k addition. More specifically, $M \in \mathbf{Z}^n$ is an n-tuple, each entry M_k of which is either ∞ or a positive natural number, indicating the cardinality of the set B in each of its n dimensions.

The set $\mathbf{P}$ is simply the set of neighbors to which each node in the grid may be connected. Condition (a) disallows self-connected elements. Condition (b) allows for automorphisms under any shifting of the nodes. Condition (c) merely simplifies our modulus-M_k additions. The $\oplus$ operator allows for indexing of neighboring nodes relative to a particular one.

Each indexed node is connected to ground through a nonlinear conductance described by $i = f_j^{(\mathbf{0})}(v)$ and to a node $j \oplus p$ by a nonlinear conductance described by $i = f_j^{(p)}(v)$. Of course, the conductance connected from j to $j \oplus p$ is the same as the conductance connected from $j \oplus p$ to j. However, since we are dealing with nonuniform grids, these conductances may vary as j and p vary. We also assume that, for each $j \in \mathbf{B}$, there is a current source h_j connected from ground to each node j such that the h_j's comprise a vector $\mathbf{h} = \{h_j : j \in \mathbf{B}\}$.

Example 1 . The infinite triangular grid shown in Figure 1 is a particular case of this structure with $n = 2$, $\mathbf{B} = \mathbf{Z}^n, \mathbf{P} = \{(1,0),(0,1),(1,1),(-1,0),(0,-1),(-1,-1)\}, \oplus$ the componentwise n-dimensional integer addition.

Example 2 . The infinite hexagonal grid shown in Figure 2 can be described by the same parameters as in Example 1. However, three of the six $f_j^{(p)}$ functions will be zero-

valued, for each j. Alternatively, the grid can be mapped into the one shown in Figure 3, which corresponds to a rectangular grid. Now only one of the four $f_j^{(p)}$ functions will be zero-valued.

Example 3 . The finite ladder network in Figure 4 is a 1-dimensional grid (n=1), with $\mathbf{B} = \{0,1,2,3,4\}, \mathbf{P} = \{1,-1\}$, and $\oplus$ is the modulus-5 sum. This forces the border nodes to be neighbors, a fact that will be useful later on.

Example 4 . The grid in Figure 5 is finite in the j_1 index (having 3 nodes in this direction) and infinite in the j_2 index. Then $j \oplus k = (j_1 + k_1(\text{mod}3), j_2 + k_2)$.

3 The Conductance Operator

We note that Kirchhoff's current law must be satisfied at each node j,

$$f_j^{(\mathbf{0})}(v_j) + \sum_{p \in \mathbf{P}} f_j^{(p)}(v_j - v_{j \oplus p}) = h_j \tag{2}$$

for all j. (Here, $f_j^{(p)} = f_{j \oplus p}^{(-p)}$).

We now express each $f_j^{(p)}(\cdot)$ and $f_j^{\mathbf{0}}(\cdot)$ as the sum of a linear component and a nonlinear one:

$$f_j^{(\mathbf{0})}(v_j) = m_{\mathbf{0}} v_j + \hat{f}_j^{(\mathbf{0})}(v_j) \tag{3}$$

and

$$f_j^{(p)}(v_j - v_{j \oplus p}) = m_p(v_j - v_{j \oplus p}) + \hat{f}_j^{(p)}(v_j - v_{j \oplus p}), \tag{4}$$

for all $p \in \mathbf{P}$, where the constants m_p and $m_{\mathbf{0}}$ are conductance coefficients and are chosen arbitrarily **but are independent of** $j \in \mathbf{B}$. The m_p's may differ for different p, except that $m_p = m_{-p}$.

The linear part represents a uniform linear grid, and the nonlinear part represents in general a **nonuniform nonlinear grid**. Equation (2) can now be rewritten as

$$\sum_{p \in \mathbf{P}} [m_p(v_j - v_{j \oplus p}) + \hat{f}_j^{(p)}(v_j - v_{j \oplus p})] + m_{\mathbf{0}} v_j + \hat{f}_j^{(\mathbf{0})}(v_j) = h_j. \tag{5}$$

for all $j \in \mathbf{B}$. Rearranging this, we obtain

$$(m_{\mathbf{0}} + \sum_{p \in \mathbf{P}} m_p) v_j - \sum_{p \in \mathbf{P}} m_p v_{j \oplus p} + \hat{f}_j^{(\mathbf{0})}(v_j) + \sum_{p \in \mathbf{P}} \hat{f}_j^{(p)}(v_j - v_{j \oplus p}) = h_j. \tag{6}$$

The first two terms of this equation are linear and combine into a matrix whose components are indexed by elements of the set $\mathbf{B} \times \mathbf{B}$. We shall refer to such a matrix as a (finite or infinite) $2n$-dimensional matrix. Let $\mathbf{y}_L$ be that matrix. It will be chosen so that it is invertible. The last two terms of (6) combine into a nonlinear operator $\mathbf{y}_N$. Now, we can write the set of equations for all j's as a single vector equation:

$$\mathbf{y}_L \mathbf{v} + \mathbf{y}_N(\mathbf{v}) = \mathbf{h}. \tag{7}$$

Here $\mathbf{v}$ and $\mathbf{h}$ are vectors of node voltages and current sources respectively. They can be treated as members of a Banach space $\mathbf{A}$ whose norm we will adjust as needed. Let us denote a vector $\mathbf{x} \in \mathbf{A}$ as $\mathbf{x} = [x_j]_j, j \in \mathbf{B}$, the x_j's being the components of $\mathbf{x}$. In our case, the elements of $\mathbf{A}$ must satisfy $\|[x_{j \oplus p}]_j\| = \|[x_j]_j\|$ for every $p \in \mathbf{P}$. The nonlinear and possibly nonuniform operator $\mathbf{y}_N : \mathbf{A} \to \mathbf{A}$ is defined by

$$\mathbf{y}_N(\mathbf{v}) = [\hat{f}_j^{(\mathbf{0})}(v_j) + \sum_{p \in \mathbf{P}} \hat{f}_j^{(p)}(v_j - v_{j \oplus p})]_j. \tag{8}$$

Equation (7) can now be rewritten as

$$\mathbf{v} + \mathbf{y}_L^{-1} \mathbf{y}_N(\mathbf{v}) = \mathbf{y}_L^{-1} \mathbf{h}. \tag{9}$$

Therefore, we have

$$\mathbf{v} = \mathbf{y}_L^{-1} \mathbf{h} - \mathbf{y}_L^{-1} \mathbf{y}_N(\mathbf{v}) = \mathbf{d}_h(\mathbf{v}). \tag{10}$$

If $\mathbf{y}_L^{-1} \mathbf{y}_N$ is a contraction on $\mathbf{A}$ then so too is $\mathbf{d}_h$, and we can find a solution using the fixed point theorem and the usual iteration for a contraction mapping on a Banach space [3, page 27].

Now consider $\mathbf{y}_N$. Let $\mathbf{w}, \mathbf{x} \in \mathbf{A}$. Then

$$\|\mathbf{y}_N(\mathbf{w}) - \mathbf{y}_N(\mathbf{x})\| = \|[\hat{f}_j^{(\mathbf{0})}(w_j) + \sum_{p \in \mathbf{P}} \hat{f}_j^{(p)}(w_j - w_{j \oplus p})]_j - [\hat{f}_j^{(\mathbf{0})}(x_j) + \sum_{p \in \mathbf{P}} \hat{f}_j^{(p)}(x_j - x_{j \oplus p})]_j\|. \tag{11}$$

Applying the triangle inequality, we have

$$\|\mathbf{y}_N(\mathbf{w})-\mathbf{y}_N(\mathbf{x})\| \leq \|[\hat{f}_j^{(\mathbf{0})}(w_j)-\hat{f}_j^{(\mathbf{0})}(x_j)]_j\|+\sum_{p\in\mathbf{P}} \|[\hat{f}_j^{(p)}(w_j-w_{j\oplus p})-\hat{f}_j^{(p)}(x_j-x_{j\oplus p})]_j\|. \quad (12)$$

We assume a Lipschitz condition on $\hat{f}_j^{(\mathbf{0})}$and $\hat{f}_j^{(p)}$uniformly for all j. In particular, we assume for all $\alpha_j, \beta_j \in \mathbf{R}$ and for all $j \in \mathbf{B}$ that

$$|\hat{f}_j^{(\mathbf{0})}(\alpha_j) - \hat{f}_j^{(\mathbf{0})}(\beta_j)| \leq \gamma_{\mathbf{0}}|\alpha_j - \beta_j| \quad (13)$$

and

$$|\hat{f}_j^{(p)}(\alpha_j) - \hat{f}_j^{(p)}(\beta_j)| \leq \gamma_p|\alpha_j - \beta_j|, \quad (14)$$

for all $p \in \mathbf{P}$. The γ_p's and $\gamma_{\mathbf{0}}$ are positive real constants. We now can write

$$\begin{aligned} \|\mathbf{y}_N(\mathbf{w}) - \mathbf{y}_N(\mathbf{x})\| &\leq \gamma_{\mathbf{0}}\|\mathbf{w} - \mathbf{x}\| + \sum_{p\in\mathbf{P}} \gamma_p\|[(w_j - x_j) - (w_{j\oplus p} - x_{j\oplus p})]_j\| \\ &\leq \gamma_{\mathbf{0}}\|\mathbf{w} - \mathbf{x}\| + 2\sum_{p\in\mathbf{P}} \gamma_p\|\mathbf{w} - \mathbf{x}\| \end{aligned} \quad (15)$$

where we make use of the triangular inequality repeatedly and also the fact that $\|[w_{j\oplus p} - x_{j\oplus p}]_j\| = \|[w_j - x_j]_j\| = \|\mathbf{w} - \mathbf{x}\|$.

Using this relation we note that $\mathbf{y}_L^{-1}\mathbf{y}_N$ satisfies a Lipschitz condition:

$$\|\mathbf{y}_L^{-1}\mathbf{y}_N(\mathbf{w}) - \mathbf{y}_L^{-1}\mathbf{y}_N(\mathbf{x})\| \leq \|\mathbf{y}_L^{-1}\|(\gamma_{\mathbf{0}} + 2\sum_{p\in\mathbf{P}} \gamma_p)\|\mathbf{w} - \mathbf{x}\|. \quad (16)$$

If

$$k = \|\mathbf{y}_L^{-1}\|(\gamma_{\mathbf{0}} + 2\sum_{p\in\mathbf{P}} \gamma_p) \quad (17)$$

is less than 1, then both $\mathbf{y}_L^{-1}\mathbf{y}_N$ and $\mathbf{d}_h$ are contractions. This allows an iterative solution for the grid in the standard way.

4 Selecting the Linear Operator

The choice of the space A and its corresponding norm depends on the grid that we are dealing with. It will also determine the choice of the linear operator.

4.1 Infinite grids

If the grid is to be infinite in all dimensions, the space A is chosen to be l^n_{2r}, the real Hilbert coordinate space with coordinates indexed by $\mathbf{Z}^n$ [6, pages 217 and 220]. This is done so that we only allow finite power regimes on the grids under consideration. The linear grid can be selected so that it is uniform, and thus $\mathbf{y}_L$ will be a 2n-dimensional Laurent matrix, defined by:

$$y_{j,j+q} = \begin{cases} m_{\mathbf{0}} + \sum_{p \in \mathbf{P}} m_p & \text{if } q = \mathbf{0}, \\ -m_q = -m_{-q} & \text{if } q \in \mathcal{P}, \\ 0 & \text{otherwise.} \end{cases} \tag{18}$$

where $j, q \in \mathbf{Z}^n$.

Let $[-\pi, \pi]^n$ denote the Cartesian product of n replicates of the real interval $[-\pi, \pi]$ and let $\theta \in [-\pi, \pi]^n$. Also, let multiplication by $Y_L(\theta)$ be the image of the operator $\mathbf{y}_L$ under the n-dimensional Fourier transformation of node-voltage vectors (See [6, Section 7.1]). Thus,

$$Y_L(\theta) = (m_0 + \sum_{p \in \mathbf{P}} m_p) - \sum_{p \in \mathcal{P}} m_p cos(p \cdot \theta), \tag{19}$$

where $(p \cdot \theta)$ denotes the dot product. Let us now choose the linear grid such that $\sum_{p \in \mathbf{P}} m_p(1 - cos(p \cdot \theta))$ may take only nonnegative or nonpositive values for all θ. A sufficient condition for this to occur is that all m_p's have the same sign. By choosing $m_{\mathbf{0}}$ to be of the same sign as the m_p's, we guarantee that $Y_L(\theta)$ is nonzero for all $\theta \in [-\pi, \pi]^n$. It then follows that $\mathbf{y}_L^{-1}$ exists and that

$$\|\mathbf{y}_L^{-1}\| = \frac{1}{\inf_\theta Y_L(\theta)} = \frac{1}{|m_0|}. \tag{20}$$

Note however that the case of passive conductances occcurs when $m_{\mathbf{0}} > 0$.

We have hereby established the following theorem:

Theorem 1 *Given an infinite n-dimensional grid characterized by the index sets* $\mathbf{B} = \mathbf{Z}^n$ *and* $\mathbf{P}$ *and a set of floating and grounding conductances, assume the following:*

1. *The linear-nonlinear decomposition of these parameters is such that* $m_{\mathbf{0}}$ *and the* m_p*'s all have the same sign; that is, the grid corresponding to the linear part of the decomposition is either passive everywhere or active everywhere.*

2. *The Lipschitz conditions given by (13) and (14) hold uniformly for all j.*

3. *The k given by (17) and (20) is less than 1.*

Then, for any input $\mathbf{h} \in l_{2r}^n$ the grid has a unique set of node voltages. That set can be found by the standard iterative procedure for a contraction mapping on l_{2r}^n.

Our next objective is to minimize the value of

$$k = \frac{\gamma_0 + 2\sum_{p\in\mathbf{P}} \gamma_p}{|m_\mathbf{0}|} \tag{21}$$

by selecting appropiate linear parts. Let $a_\mathbf{0}$ and a_p be the infima of the slopes of all the chords of all the $f_j^{(\mathbf{0})}$ and all the $f_j^{(p)}$ respectively. These are finite by our assumption of uniform Lipschitz conditions. Similarly, let $b_\mathbf{0}$ and b_p be the corresponding suprema, also finite.

We will first minimize each γ_p ($p \in \mathbf{P}$) by selecting a suitable m_p. A little reflection will show that we need only search for our m_p in the range $[a_p, b_p]$ to find the minimal γ_p. Inside this range, we have that, for any given $m_p \in [a_p, b_p]$,

$$\gamma_p = \max(b_p - m_p, m_p - a_p). \tag{22}$$

We are still free to adjust m_p to make γ_p as small as possible. A graph of γ_p as a function of m_p will consist of the upper portion of the union of two straight lines, with slopes of ± 1 (See Figure 6). The intersection of these lines will yield the value of m_p for which γ_p takes its minimum value. This occurs when the two terms in the right hand side of (22) are equal; i.e., when

$$m_p = \frac{1}{2}(a_p + b_p). \tag{23}$$

In this case,

$$\gamma_p = \frac{1}{2}(b_p - a_p). \tag{24}$$

By choosing γ_p in accordance with (24), we minimize the summation in (21). We can still manipulate γ_0 and $m_\mathbf{0}$ in order to minimize k still further. Let $s = 2\sum_{p\in\mathbf{P}} \gamma_p$. Note that $s > 0$. Equation (21) can be rewritten as

$$k = |m_0|^{-1}(\max(b_\mathbf{0} - m_\mathbf{0}, m_\mathbf{0} - a_\mathbf{0}) + s) \tag{25}$$

Again, we use the fact that the max(...) term is the union of two segments of straight lines with slopes of different signs as in Figure 2, but with m_p replaced by m_0. We then can write:

$$k = \begin{cases} |m_0|^{-1}(b_0 - m_0 + s) & \text{if } a_0 \leq m_0 \leq \frac{1}{2}(a_0 + b_0) \\ |m_0|^{-1}(s + m_0 - a_0) & \text{if } \frac{1}{2}(a_0 + b_0) \leq m_0 \leq b_0 \end{cases} \tag{26}$$

From now on, m.i. and m.d. will denote a monotically increasing and a monotonically decreasing function of m_0 respectively. We will also denote the two items in equation (26) by k_1 and k_2 respectively. Consider k as a function of m_0. There are four possible cases:

- $a_0 < b_0 < 0$. In this case, $k_1 = 1 + |m_0|^{-1}(b_0 + s)$ and $k_2 = -1 + |m_0|^{-1}(s - a_0)$. k_2 is m.i. in $[a_0, b_0]$. If $s + b_0 \geq 0$, then k_1 is m.i., and, since k is a continuous function of m_0, then $k > 1$ for all m_0. We therefore need $s + b_0 < 0$ (i.e., $s < -b_0$) to have a contraction. In this case, k_1 is m.d. and bounded above by $+1$. By solving $k_2 < 1$ for m_0 we get $m_0 < \frac{1}{2}(a_0 - s)$. The minimal k will correspond to $m_0 = \frac{1}{2}(a_0 + b_0)$.

- $a_0 < 0, b_0 > 0$. In this case, $k_1 = |m_0|^{-1}(b_0 + s) - \text{sgn}(m_0)$ and $k_2 = |m_0|^{-1}(s - a_0) + \text{sgn}(m_0)$. We note that $k_1 > 1$ for $m_0 > 0$ and $k_2 > 1$ for $m_0 < 0$. We know that k_1 and k_2 must intersect; the value of k will never be less than 1 for this case.

- $0 < a_0 < b_0$. In this case, $k_1 = -1 + |m_0|^{-1}(b_0 + s)$ and $k_2 = 1 + |m_0|^{-1}(s - a_0)$. Now k_1 is m.i. If $s - a_0 \geq 0$ then $k_2 > 1$ for all m_0. We therefore need $s - a_0 < 0$ (i.e., $s < a_0$) to have a contraction. In this case, k_2 is m.d. and bounded above by $+1$. By solving $k_1 < 1$ we get $m_0 < \frac{1}{2}(s + b_0)$. Again the minimal k will correspond to $m_0 = \frac{1}{2}(a_0 + b_0)$.

We have established the following:

Corollary 1 *Given a grid with conditions established in Theorem 1, let a_0 and b_0 be lower and upper bounds on the slopes of the i-v characteristic curves of the grounding elements. Also, let $s = 2\sum_{p \in \mathbf{P}} \gamma_p$, where the γ_p's are the Lipschitz constants for the floating elements. A necessary condition for the existence of a unique current voltage regime is that the grounding elements are either totally active or totally passive. Moreover, if the elements are totally active, we must have $s < -b_0$, and, if the elements are totally passive, we must have $s < a_0$.*

4.2 Finite Grids

Physical systems on the one hand and numerical computations on the other require that the number of nodes be finite. The infinite-grid analysis above presented can be modified slightly to encompass this case. The binary operator $\oplus$ implies some kind of wrap-around condition in the finite grid. In example 2 above, this wrap-around happens at the boundary of the 1-dimensional grid. Also, we will have a choice on the norm of our vector space, which will induce a particular norm on the linear operator.

The space A will consist of n-dimensional finite vectors of real components. There are various norms that can be used in this space. We will consider the $\|\cdot\|_2$ norm.

If the grid under consideration is finite, the $\mathbf{y}_L$ operator will be a finite 2n-dimensional matrix. Since the linear parts are chosen uniformly, they form a circulant matrix [5]. This means that our linear grid wraps around its boundaries. This fact will be useful for numerical computations. Also, if $\mathbf{y}_L$ is circulant, then $\mathbf{y}_L^{-1}$ is also circulant.

Of course, real grids usually do not have this wrap-around characteristic. In fact, if we go back to Example 2, the $f_4^1(\cdot)$ function must be zero throughout its domain in order to remove the wrap-around conductance. This is not a problem in our scheme since the nonlinear part can be made to be the negative of the linear part, thus giving us the necessary "open-circuit" connection. In the example, this means that $\hat{f}_4^{(1)}(v) = \hat{f}_0^{(-1)}(v) = -m_1 v$.

We can now find the norm of the inverse of the linear operator.

Lemma 1 *Let $\mathbf{y}_L$ be the circulant matrix corresponding to the finite linear grid. Assume that $m_0 \neq 0$ and that it has the same sign as all of the m_p's. We then have*

$$\|\mathbf{y}_L^{-1}\| = \frac{1}{|m_0|} \tag{27}$$

PROOF: For simplicity, we will assume a 1-dimensional grid. Therefore y_L is 2-dimensional. Let c be the cardinality of **B**. Let the rows and columns of $\mathbf{y}_L$ be indexed from 0 to $c-1$ and let $a_{i,k}$ be an element of the matrix. The eigenvalues of $\mathbf{y}_L$ are $\lambda_l = \sum_{k=0}^{c-1} a_{0,k}\omega_l^k$, $l = 0, 1, \ldots, c-1$, where $\omega_l = e^{2\pi\sqrt{-1}/c}$ is a root of unity [5]. Since $m_0 \neq 0$, no eigenvalues are zero. Therefore $\mathbf{y}_L^{-1}$ exists.

According to [5] we have that this matrix is diagonizable, that is $\mathbf{y}_L^{-1} = SD^{-1}S^{-1} = \frac{1}{c}SD^{-1}S^*$, where S is a Vandermonde matrix whose elements are roots of unity, S^* is its

complex conjugate transpose, and D is the matrix with diagonal entries corresponding to the eigenvalues. Since none of the eigenvalues are zero, D^{-1} is a diagonal matrix whose elements are the inverses of D. Let us denote a matrix A by $[a_{i,k}]_{i,k}$ where the $a_{i,k}$ are the elements indexed by i and j. Then $S = [\omega_j^i]_{i,j}$, $S^* = [\overline{\omega}_i^j]_{i,j}$, and $D^{-1} = [d_i\delta_{i,j}]_{i,j}$, where $d_i = \lambda_i^{-1}$ and $\delta_{i,j}$ is the Kronecker delta.

We have that:

$$\begin{aligned} y_L^{-1} &= \frac{1}{c} S D^{-1} S^* \\ &= \frac{1}{c}[\sum_{k=0}^{c-1} \omega_k^i d_k \delta_{k,j}]_{i,j} S^* \\ &= \frac{1}{c}[\omega_j^i d_j]_{i,j}[\overline{\omega}_i^j]_{i,j} \\ &= \frac{1}{c}[\sum_{k=0}^{c-1} \omega_k^i d_k \overline{\omega}_k^j]_{i,j} \end{aligned}$$

and therefore,

$$(y_L^{-1})^* = \frac{1}{c}[\sum_{k=0}^{c-1} d_k \overline{\omega}_k^i \omega_k^j]_{i,j}$$

where the eigenvalues are all real given the symmetric nature of y_L. Consider $T = (y_L^{-1})^* y_L^{-1}$:

$$\begin{aligned} T &= \frac{1}{c^2}[\sum_{l=0}^{c-1} d_l \omega_l^j \overline{\omega}_l^i]_{i,j}[\sum_{m=0}^{c-1} d_m \omega_m^i \overline{\omega}_m^j]_{i,j} \\ &= \frac{1}{c^2}[\sum_{k=0}^{c-1}(\sum_{l=0}^{c-1} d_l \omega_l^k \overline{\omega}_l^i)(\sum_{m=0}^{c-1} d_m \omega_m^k \overline{\omega}_m^j)]_{i,j} \end{aligned}$$

The fact that y_L is symmetric makes all the entries in the derived matrices to be real. The fact that the m_{ω} and m_p's all have the same sign means that the entries of T are all positive. This also means that the largest eigenvalue of T, as defined in [5] will be λ_0, i.e. the sum over any row or column. Then, $\|y_L^{-1}\| = (\max\{\text{eigenvalues of T}\})^{1/2} = \sqrt{\lambda_0\{T\}}$ [4].

$$\begin{aligned} \lambda_0\{T\} &= \sum_{j=0}^{c-1} \frac{1}{c^2} \sum_{k=0}^{c-1}(\sum_{l=0}^{c-1} d_l \omega_l^k)(\sum_{m=0}^{c-1} d_m \omega_m^k \overline{\omega}_m^j) \\ &= \frac{1}{c^2} \sum_{j=0}^{c-1} \sum_{k=0}^{c-1} \sum_{l=0}^{c-1} \sum_{m=0}^{c-1} d_l d_m \omega_l^k \omega_m^k \overline{\omega}_m^j \end{aligned}$$

$$= \frac{1}{c^2}\sum_{j=0}^{c-1}\sum_{k=0}^{c-1} d_0 d_0 \omega_0^k \omega_0^k \overline{\omega}_0^j + \frac{1}{c^2}\sum_{j=0}^{c-1}\sum_{k=0}^{c-1}\sum_{l=1}^{c-1}\sum_{m=1}^{c-1} d_l d_m \omega_l^k \omega_m^k \overline{\omega}_m^j$$

$$= \frac{1}{c^2}\sum_{j=0}^{c-1}\sum_{k=0}^{c-1} d_0^2 + \frac{1}{c^2}\sum_{l=1}^{c-1}\sum_{m=1}^{c-1} d_l d_m \sum_{j=0}^{c-1} \omega_l^k \omega_m^k \sum_{k=0}^{c-1} \overline{\omega}_m^j$$

The first term simply sums to d_0^2. The last sum in the last term is always zero, so $\lambda_0\{T\} = d_0^2$. Therefore $\|y_L^{-1}\| = \sqrt{\lambda_0\{T\}} = |d_0| = 1/|\lambda_0\{y_L\}| = 1/|m_0|$. Q.E.D.

By virtue of Lemma 1 and an adaptation of our prior arguments, we can establish a theorem analogous to Theorem 1.

Theorem 2 *Given a finite n-dimensional grid characterized by the index sets* **B** *and* **P** *and and a set of floating and grounding conductances, assume that:*

1. *The grid is decomposed into a uniform circulant linear grid plus a nonuniform nonlinear one. The linear circulant grid is such that it is either passive everywhere or active everywhere.*

2. *The Lipschitz conditions given by (13) and (14) hold uniformly for all* $j \in \mathbf{B}$.

3. *The k given by (17) and (27) is less than 1.*

Then, for any input current distribution **h** *the grid has a unique set of node voltages. This set can be found by the standard iteration.*

Corollary 1 needs no change in the wording for it to be applicable to finite grids.

By choosing our linear operator to be a 2n-dimensional circulant matrix, we can work instead with the n-dimensional FFT of it. This reduces storage requirements significantly. Also, the FFT of $\mathbf{y}_L^{-1}$ can be computed directly from the FFT of $\mathbf{y}_L$ so that no matrix inversion is necessary at all. The FFT of y_L^{-1} will simply be the inverse (element-wise) of the FFT corresponding to the y_L circulant matrix, which is generated by the values of m_0 and the m_p's only, and needs to be calculated only once. The iteration will be:

$$\mathbf{v} = F^{-1}(F(\mathbf{y}_L^{-1})(F(\mathbf{h} - \mathbf{y}_N(\mathbf{v})) \tag{28}$$

where F, F^{-1} represent the FFT and inverse FFT respectively. The only value that need updating after each iteration is $\mathbf{y}_N(v)$, which takes as argument the previous value. The

sufficiency conditions guarantee that this iterative procedure can get arbitrarily close to the actual operating point due to the input sources.

Example 5 . Consider a 64x64 2-dimensional rectangular grid. We have that $P = \{(1,0),(-1,0),(0,1),(0,-1)\}$. The grid is indexed along rows and columns from 1 to 64. The grounding conductance function is linear, and has a value of 1. The floating conductances are uniform inside the boundaries of the grid and will be characterized by $f_j^{(p)}(v) = \tanh(v)$. Since the grid is finite, there will be nonuniformity on the boundary node connections to their neighbors. We will select $m_0 = 1$ and $m_p = 1$ for all p. Suppose an input such as the one shown in Figure 7 is applied. Figure 8 shows the first iteration (corresponding to an entirely linear grid, with wrap-around). Figure 9 shows the fourth iteration, very close to the actual operating point.

Example 6 . Take the same grid as in Example 5. Now let the original input be corrupted by random noise, as shown in Figure 10. The first iteration is shown in Figure 11. The fourth iteration is shown in Figure 12.

References

[1] A. Brown and P.R. Halmos, *Algebraic properties of Toeplitz operators*, J. für Math., 213 pp. 89-102, 1963.

[2] Christof Koch and Hua Li, *Vision Chips*, IEEE Computer Society Press, Los Alamitos, CA, 1995.

[3] L.A. Liusternik and V.J. Sobolev, *Elements of Functional Analysis*, F. Ungar Pub., New York 1961.

[4] Ben Noble, *Applied Linear Algebra*, Prentice-Hall, Englewood Cliffs, NJ, 1969.

[5] G.E. Trapp, *Inverses of Circulant Matrices and Block Circulant Matrices*, Kyungpook Math J., 13 pp 11-20, 1973.

[6] A.H. Zemanian, *Infinite Electrical Networks*, Cambridge University Press, New York, 1991.

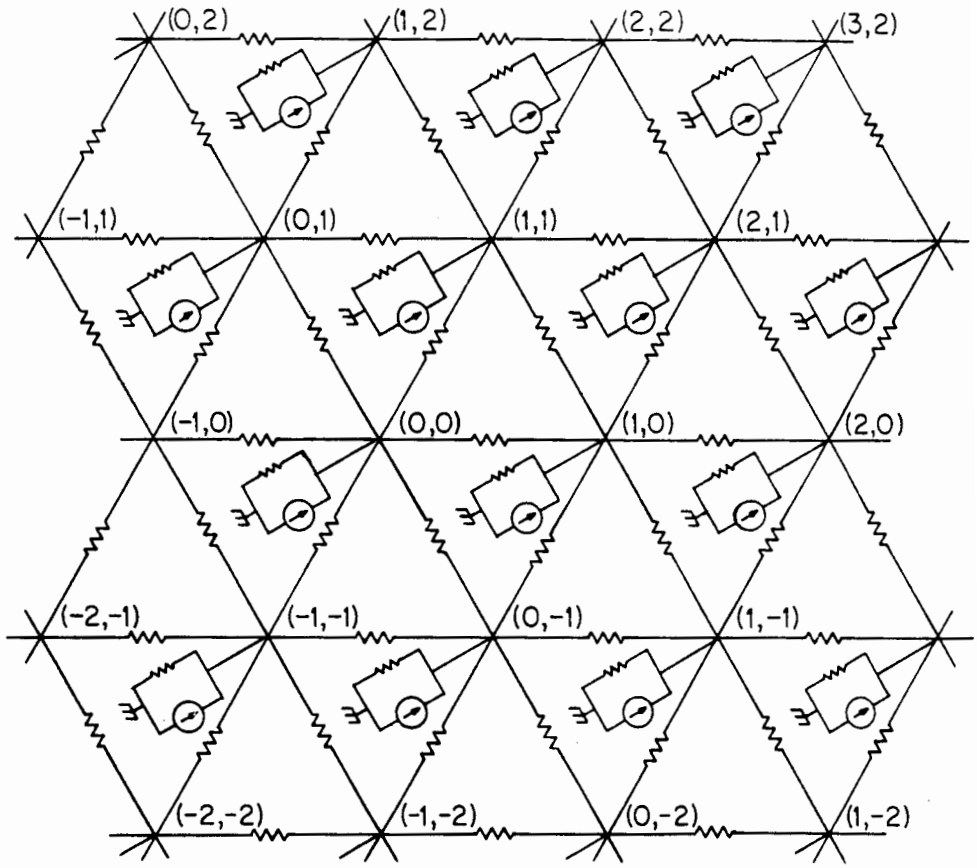

FIG. 1

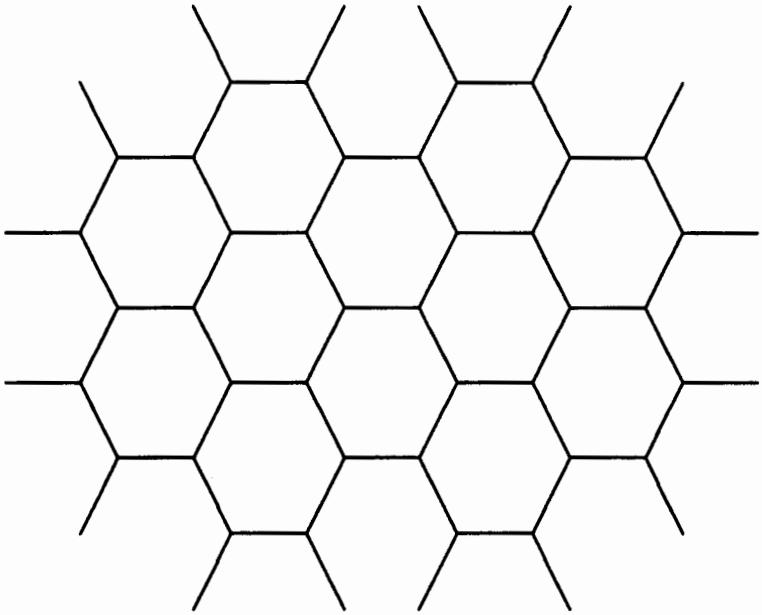

Figure 2. Portion of a graph corresponding to the infinite hexagonal grid. Not shown are the grounding conductances and current sources connecting each node to ground.

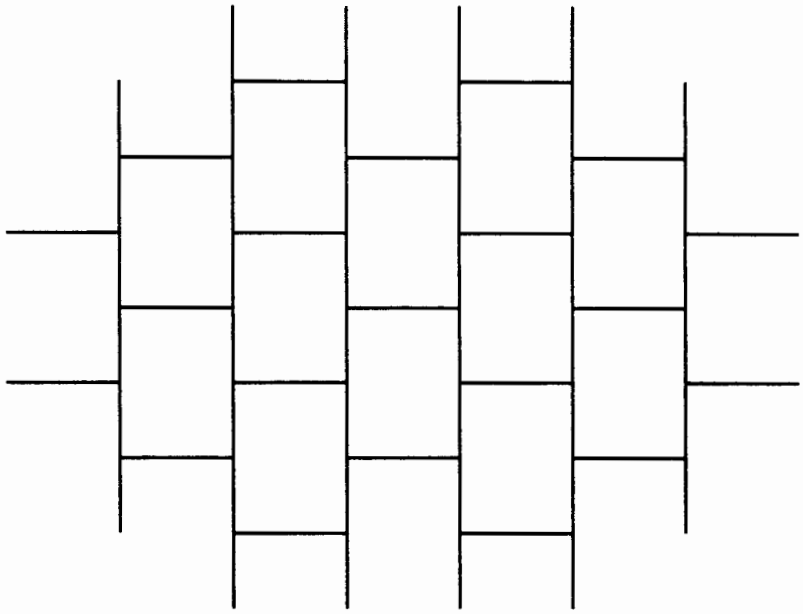

Figure 3. Portion of another graph corresponding to the infinite hexagonal grid. As was done before, the edges corresponding to conductances and current sources connecting each node to ground are not shown.

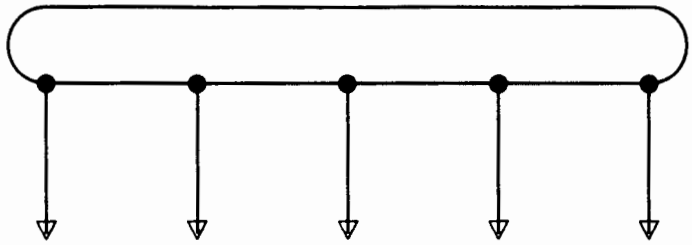

Figure 4. Graph of a finite 1-dimensional grid. Each horizontal edge represents a floating conductance. Each vertical edge represents the parallel combination of a current source and a grounding conductance, both connected to ground.

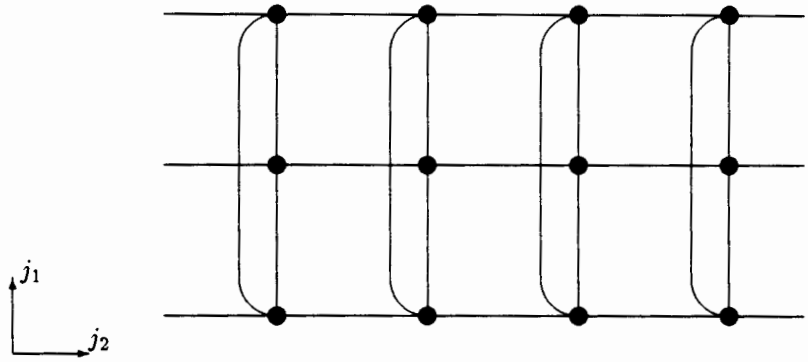

Figure 5. Section of a graph of a 2-dimensional grid. The grid is finite in the j_1 direction and infinite in the j_2 direction. Once again, the connections from each node to ground are not shown, for simplicity.

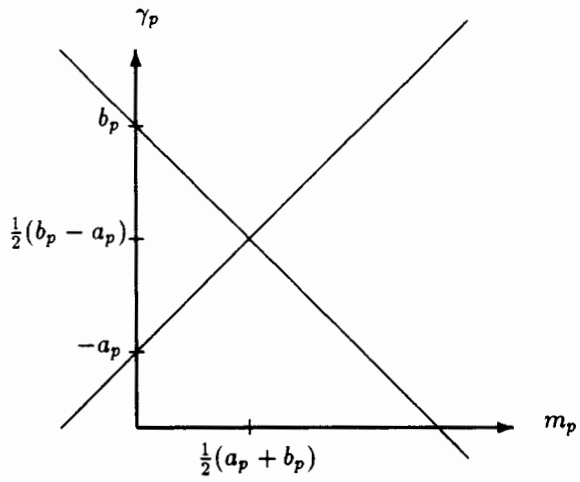

Figure 6. Plot of γ_p as a function of m_p.

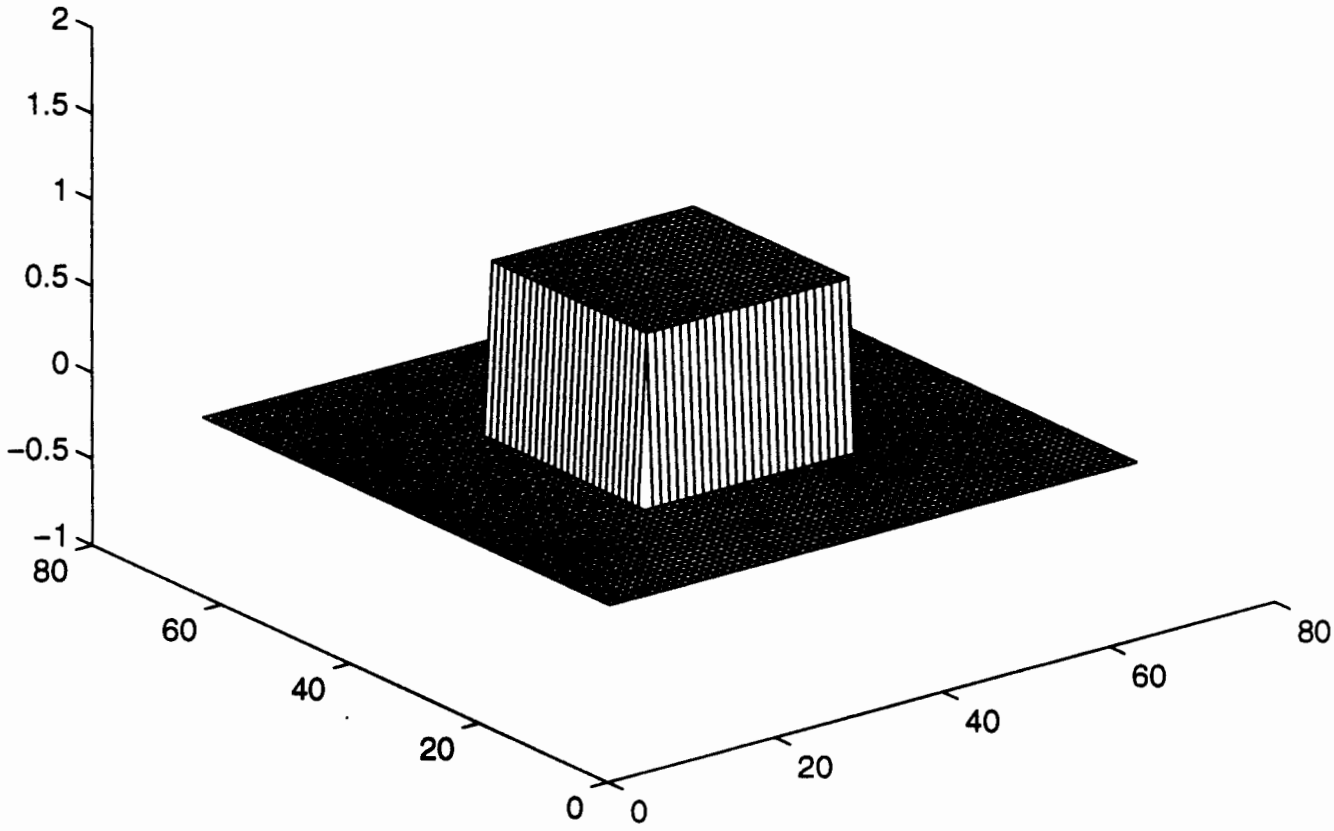

Figure 7

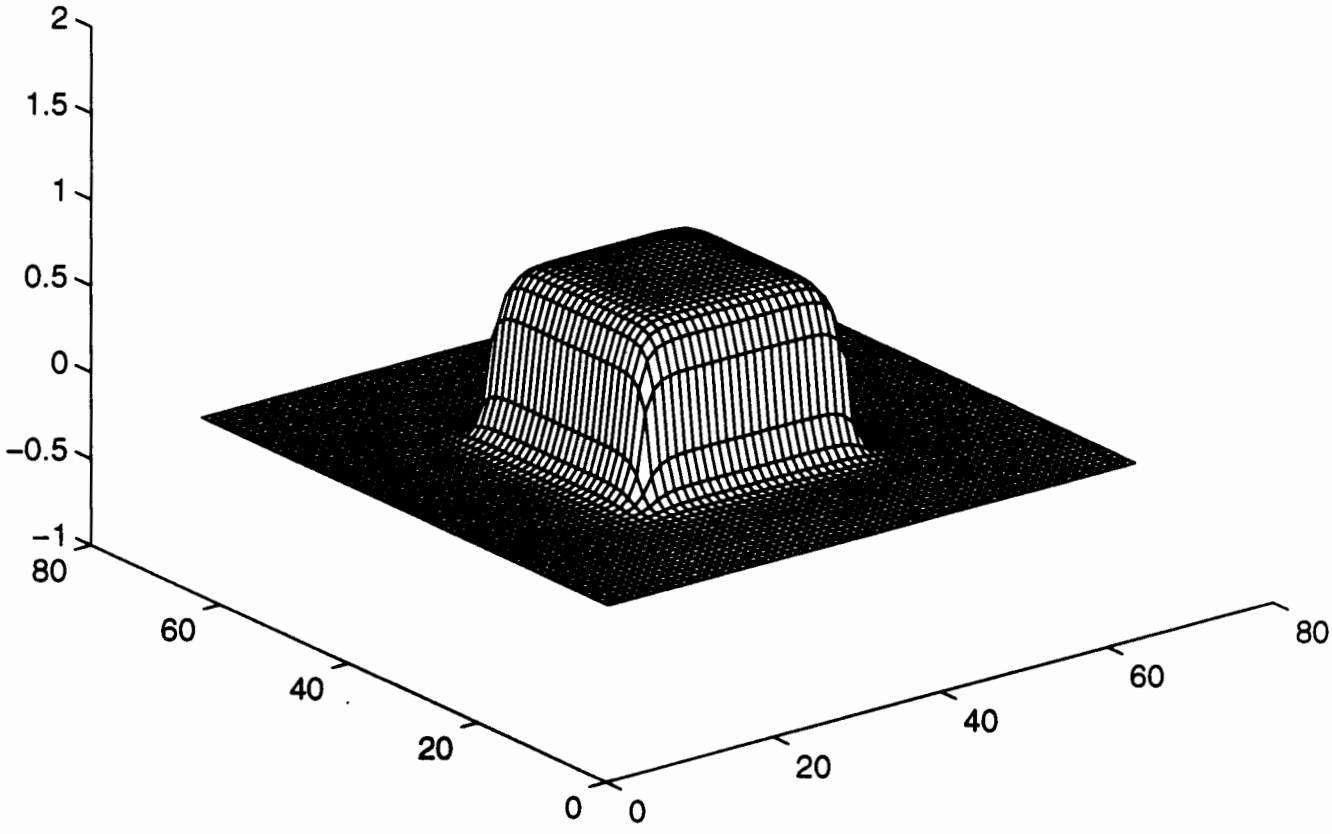

Figure 8

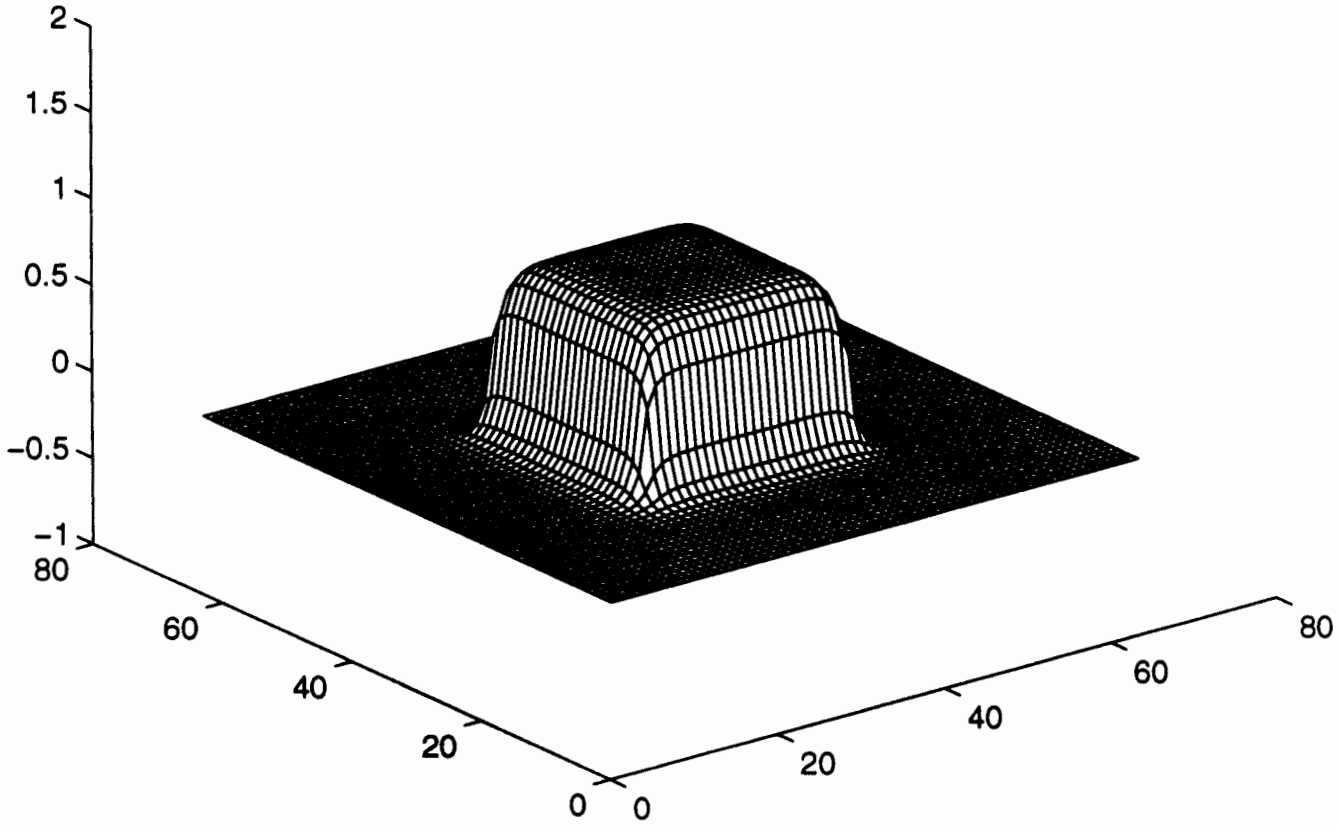

Figure 9

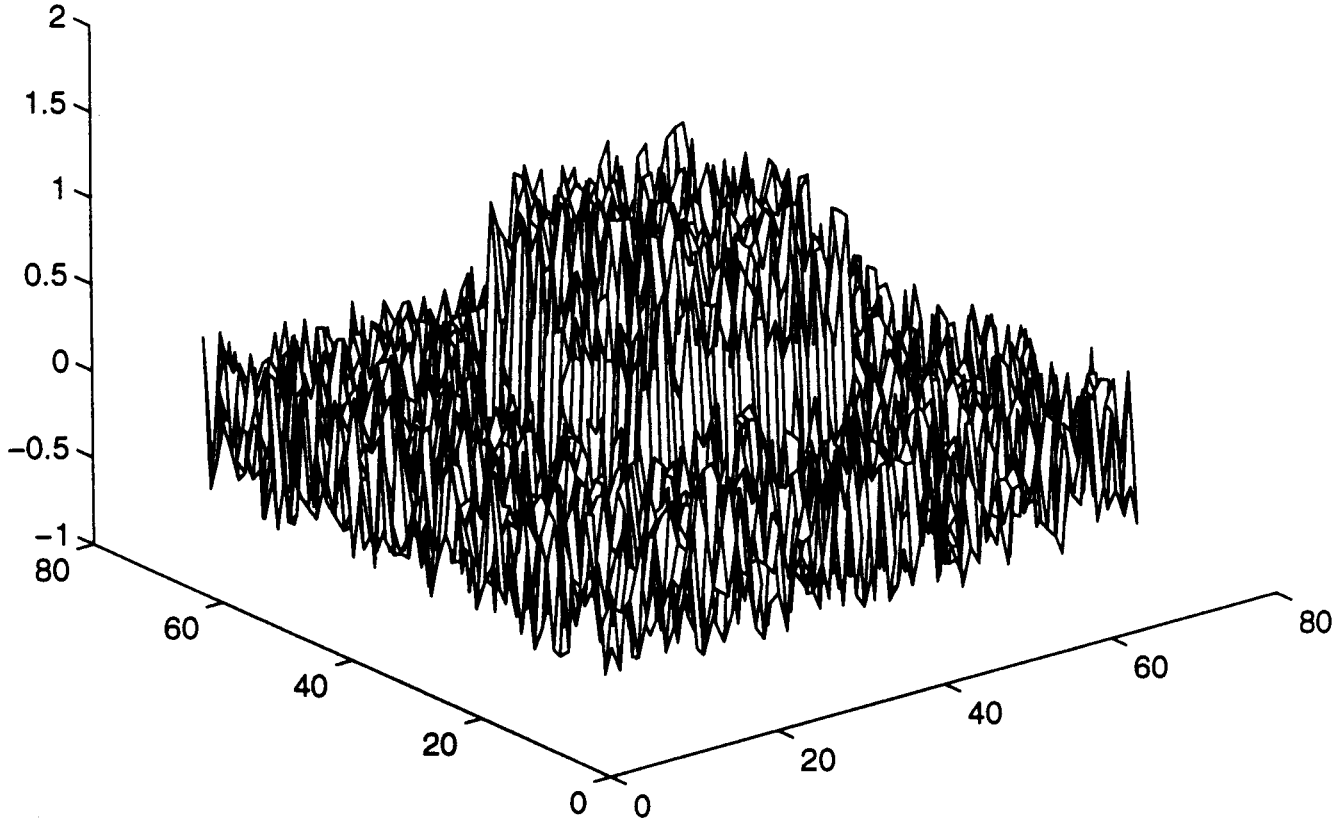

Figure 10

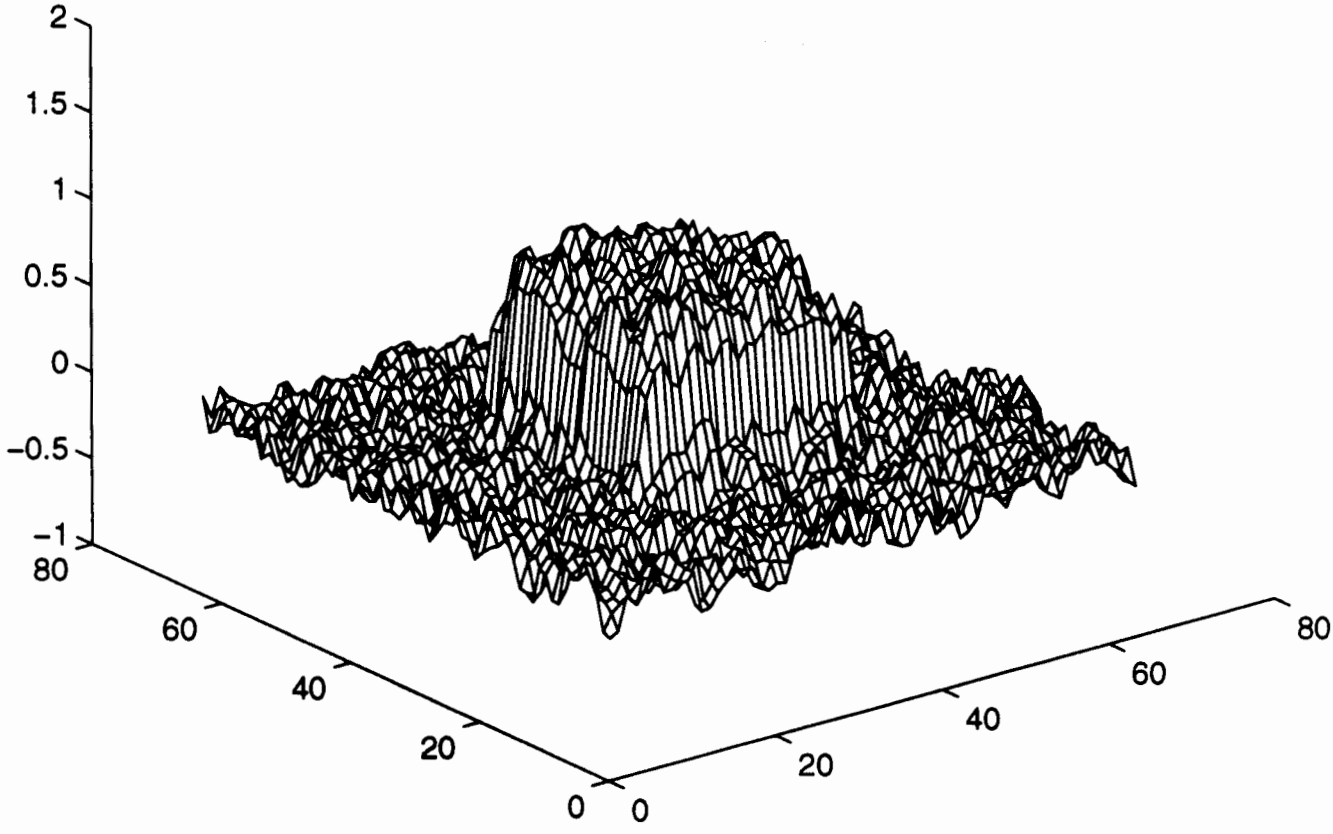

Figure 11

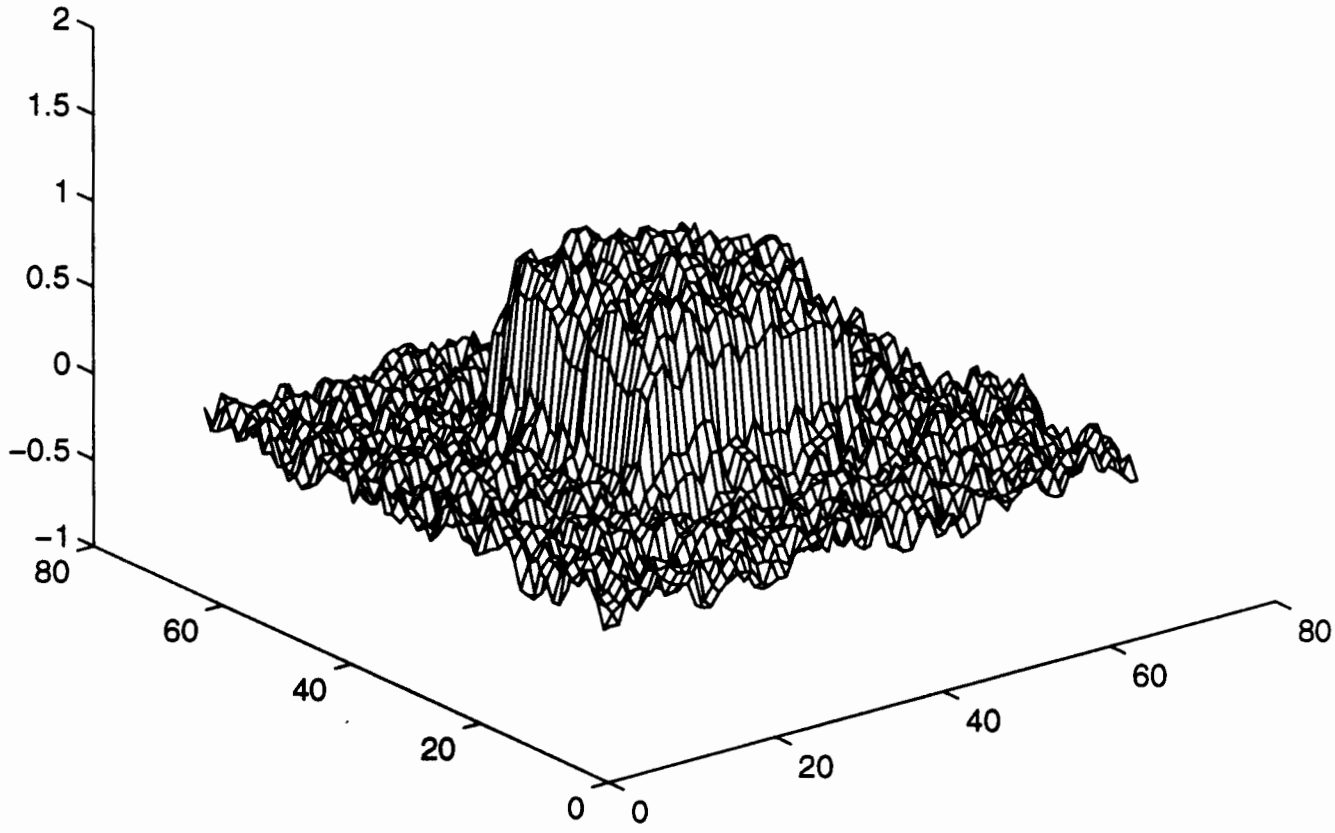

Figure 12

Figure Captions

Figure 1 .

Figure 2 . Portion of a graph of the hexagonal grid.

Figure 3 . Portion of another graph of the hexagonal grid.

Figure 4 . Graph of a finite 1-dimensional grid.

Figure 5 . Section of a graph of a 2-dimensional grid.

Figure 6 . Plot of γ_p as a function of m_p.

Figure 7 .

Figure 8 .

Figure 9 .

Figure 10 .

Figure 11 .

Figure 12 .